Organic & Biomolecular Chemistry

PAPER

View Article Online
View Journal | View Issue

Cite this: *Org. Biomol. Chem.*, 2015, **13**, 5475

Tricyclic dihydrobenzoxazepine and tetracyclic indole derivatives can specifically target bacterial DNA ligases and can distinguish them from human DNA ligase I†

Nisha Yadav,‡[a] Taran Khanam,‡[b] Ankita Shukla,[b] Niyati Rai,[b] Kanchan Hajela*[a] and Ravishankar Ramachandran*[b]

Received 5th March 2015,
Accepted 31st March 2015

DOI: 10.1039/c5ob00439j

www.rsc.org/obc

DNA ligases are critical components for DNA metabolism in all organisms. NAD^+-dependent DNA ligases (LigA) found exclusively in bacteria and certain entomopoxviruses are drawing increasing attention as therapeutic targets as they differ in their cofactor requirement from ATP-dependent eukaryotic homologs. Due to the similarities in the cofactor binding sites of the two classes of DNA ligases, it is necessary to find determinants that can distinguish between them for the exploitation of LigA as an anti-bacterial target. In the present endeavour, we have synthesized and evaluated a series of tricyclic dihydrobenzoxazepine and tetracyclic indole derivatives for their ability to distinguish between bacterial and human DNA ligases. The *in vivo* inhibition assays that employed LigA deficient *E. coli* GR501 and *S. typhimurium* LT2 bacterial strains, rescued by ATP-dependent T4 DNA ligase or *Mycobacterium tuberculosis* NAD^+-dependent DNA ligase (Mtb LigA), respectively, showed that the compounds can specifically inhibit bacterial LigA. The *in vitro* enzyme inhibition assays using purified MtbLigA, human DNA ligase I & T4 DNA ligase showed specific inhibition of MtbLigA at low micromolar range. Our results demonstrate that tricyclic dihydrobenzoxazepine and tetracyclic indole derivatives can distinguish between bacterial and human DNA ligases by ~5-folds. *In silico* docking and enzyme inhibition assays identified that the compounds bind to the cofactor binding site and compete with the cofactor. Ethidium bromide displacement and gel-shift assays showed that the inhibitors do not exhibit any unwanted general interactions with the substrate DNA. These results set the stage for the detailed exploration of this compound class for development as antibacterials.

Introduction

The development of resistance to bacterial infections is an emergent issue and we need to stay one step ahead of the game. The fight includes the discovery of antibacterials with new modes of action that can presumably avoid the present evasion tactics developed by bacterial pathogens. In infectious diseases like tuberculosis that affect a huge number of the world's population, it has become even more pressing. For example, the combat against TB is protracted by the emergence of multidrug resistant (MDR) and extensively drug resistant (XDR) strains of *M. tuberculosis*[1] and comparative stagnation in the development of new antibiotics, particularly those that have novel modes of action.[2,3] Antibiotics in current use predominantly target a minuscule number of bacterial targets, largely affecting peptidoglycan, biosynthesis or gene expression/translation.[4] However, the growing body of scientific evidences suggest that there remain many cellular targets, essential for the mycobacterial pathogen, which can be evaluated for therapeutic interference.

DNA metabolism is essential for bacterial survival, and it involves indispensable processes like DNA replication, DNA recombination, DNA repair and transcription. Under the 'common enzyme-diverse pathways' approach, there may be various opportunities for novel therapeutic interventions affecting one critical functional component that influences more than one vital life processes in the microbe.[5] One such

[a]*From Medicinal and Process Chemistry, CSIR-Central Drug Research Institute, Sector10, Jankipuram Extension, Sitapur Road, Uttar Pradesh, Lucknow-226031, India. E-mail: kanchan_hajela@cdri.res.in; Fax: +91-522-2771941; Tel: +91-522-2771940*

[b]*From the Molecular and Structural Biology Division, CSIR-Central Drug Research Institute, Sector10, Jankipuram Extension, Sitapur Road, Uttar Pradesh, Lucknow-226031, India. E-mail: r_ravishankar@cdri.res.in; Fax: +91-522-2771941; Tel: +91-522-2771940*

†Electronic supplementary information (ESI) available. See DOI: 10.1039/c5ob00439j

‡These authors contributed equally to the paper.

central target is DNA ligase that catalyzes the joining of nicks between the adjoining bases of duplex DNA at a single or double stranded break by mediating the formation of phosphodiester bonds between adjacent 5′ phosphoryl and 3′ hydroxyl groups. The first step is the formation of a covalent DNA ligase-adenylate intermediate, wherein the AMP group is derived from the covalently bound cofactor that can be ATP or NAD^+.[6] Subsequently, AMP is transferred from DNA ligase to the 5′ phosphate of the nicked DNA through a pyrophosphate bond. Finally, a phosphodiester bond is formed to join adjacent polynucleotides, with the release of AMP. DNA ligases are grouped into two classes based on the source of the AMP cofactor: NAD^+-dependent DNA ligases present in bacteria, some entomopoxviruse and mimi virus and ATP-dependent DNA ligases found in different viruses, archaea, eukaryotes and higher organisms.[7–9]

NAD^+-dependent DNA ligase (LigA) has drawn attention in the case of *Mycobacterium* as a target with the potential to combat multiple drug resistances because of its essential nature for bacterial viability, high conservation and discrete nature in terms of its architecture and cofactor requirement from the human homolog.[7,10–17] The information gained by the structural studies of several DNA ligases in complex with their cofactors from prokaryotic and eukaryotic origins show many similarities in the cofactor (ATP/NAD^+) binding mode.[15,17–21] *Escherichia coli* DNA LigA structure in complex with AppDNA[22] and structure of *Enterococcus faecalis* LigA[15] with NAD^+ has underscored the existence of a "druggable" active site harbouring hydrophobic tunnel, extending from the nucleotidyl transferase domain to the adenosine-binding domain. In contrast, this tunnel is absent in ATP-dependent DNA ligase, including human DNA ligase (HuLigI).[23] This subtle difference between the host and pathogen enzymatic machinery provides a platform for the development of specific and potent antibacterials targeting the druggable tunnel. This has prompted the rational design of small molecule inhibitors to find new prototypes that can act specifically against bacterial NAD^+-dependent DNA ligases.[24–28] Arylamine compounds and chloroquine derivatives are potent LigA inhibitors but they have the disadvantage of binding to DNA. Moreover, they do not compete with NAD^+ binding and instead bind at some other target site.[29] In addition, pyridochromanones are competitive inhibitors of the enzyme.[30] Considering the employment of human DNA ligase as an anti-cancer target in recent times,[24,31–33] an anticipated challenge would be to distinguish between pathogen and host enzyme.

Our group has reported the identification of diverse compound families, which inhibit bacterial NAD^+-dependent DNA ligases with several fold specificity compared to ATP-dependent ligases, including the human DNA ligase I.[17,34,35] We have previously reported through virtual screening, *N*-substituted tetracyclic indole as a specific and potent inhibitor of NAD^+ dependent DNA ligase.[34] As part of our extended efforts, we have synthesised a new series of tetracyclic compounds (indole and dihydrobenzoxazepine derivatives) with better predicted binding affinities based partially on the position of the water clusters.[34] We have evaluated the compounds for their potencies and cofactor specificities using a variety of *in vitro* assays, involving purified enzymes, and *in vivo* assays, involving LigA deficient bacterial strains. The docking and modelling studies attribute the inhibitor specificity to the mimicking of NAD^+-enzyme interaction. Overall, the *in vitro* and *in vivo* assays clearly demonstrate that these compounds can distinguish between NAD^+ and ATP-dependent ligases and also that the *in vivo* mode of action is largely through the inhibition of the essential LigA.

Results and discussion

Chemistry

Three prototypes of compounds with different tricyclic and tetracyclic ring systems were synthesised and evaluated for their MtbLigA inhibitory activity. For the synthesis of prototype-**I**, as shown in Scheme 1, the tetracyclic indoles, namely, benzo[2,3]thiepino[4,5-*b*]indole, benzo[2,3]oxepino[4,5-*b*]-indole and benzo[6,7]cyclohepta[1,2-*b*]indole **3a–c**, which formed the core intermediates, were prepared by subjecting the phenyl hydrazones **2a–c** to Fisher indole synthesis.[36] *N*-Alkylation with commercially available 6-bromo-1,2-epoxyhexane **4** furnished the epoxides **5a–c** as solids in quantitative yields. Finally, the opening of the epoxide ring with different secondary amines gave the desired target molecules **6–28** in good yields. All the final molecules were adequately characterised by spectral analysis.

The synthesis of *N*-alkylated dibenzoxazepine derivatives (prototype **II**) was commenced with the preparation of 5,11-dihydrodibenzo[*b*,*e*][1,4]oxazepine[37] **31**. Base catalysed alkylation of 2-nitrophenol with 2-bromo benzyl bromide in dry acetone under reflux conditions afforded benzyl ether **29** in quantitative yield. Subsequent reduction of the 2-nitro group to 2-amino benzyl ether **30** followed by intramolecular CuI/L-proline catalysed C–N coupling reaction yielded dibenzoxepine **31** in 50% yield. The sequential *N*-alkylation with 6-bromo-1,2-epoxyhexane **4** followed by ring opening with different secondary amines (Scheme 2) provided the desired *N*-substituted dibenzoxepine derivatives **33–40** in excellent yields.

To synthesise the starting precursor, 10,11-dihydrodibenzo-[*b*,*f*][1,4]oxazepine[38] **43** for the synthesis of prototype **III** compounds (Scheme 3) was followed. *N*-acylation of 2-amino phenol with 2-fluoro-benzoyl chloride formed 2-fluoro-*N*-(2-hydroxyphenyl)benzamide **41**, which on etherification afforded the keto compound, dibenzo[*b*,*f*][1,4]oxazepin-11-(10*H*)-one **42** in very good yields. Subsequent reduction of the amidic carbonyl with LAH provided the cyclised oxazepine **43**, in excellent yield. Following the procedure of *N*-alkylation as described in Schemes 1 and 2, the target compounds **45–48** of prototype **III** were obtained in good to excellent yields (Scheme 3).

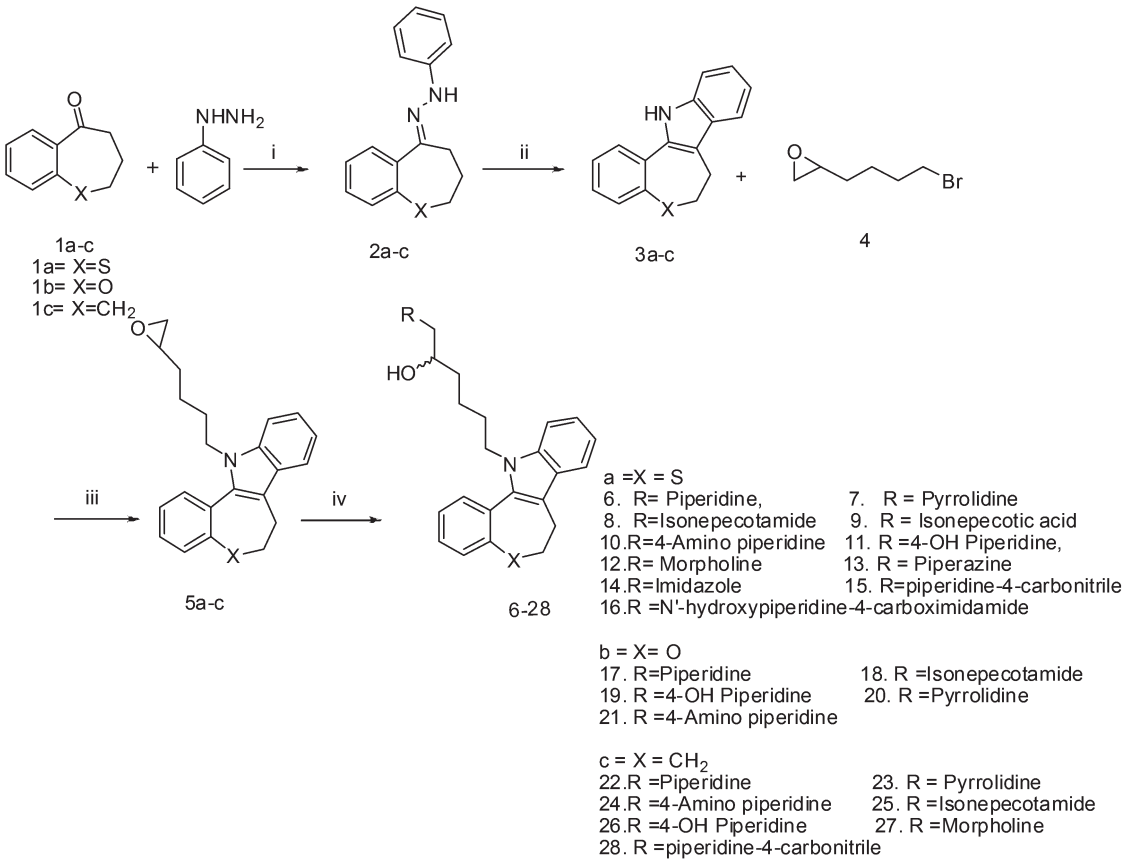

Scheme 1 Synthesis of prototype I compounds. Reagents and conditions: (i) ethanol/glc. acetic acid, reflux 6 h; (ii) EtOH, 20% aq. HCl, 80–85%; (iii) NaH, 4, dry DMF, 0 °C, RT, 1 h, 85–90%; (iv) 2° amine, EtOH, reflux, 12 h, 70–78%.

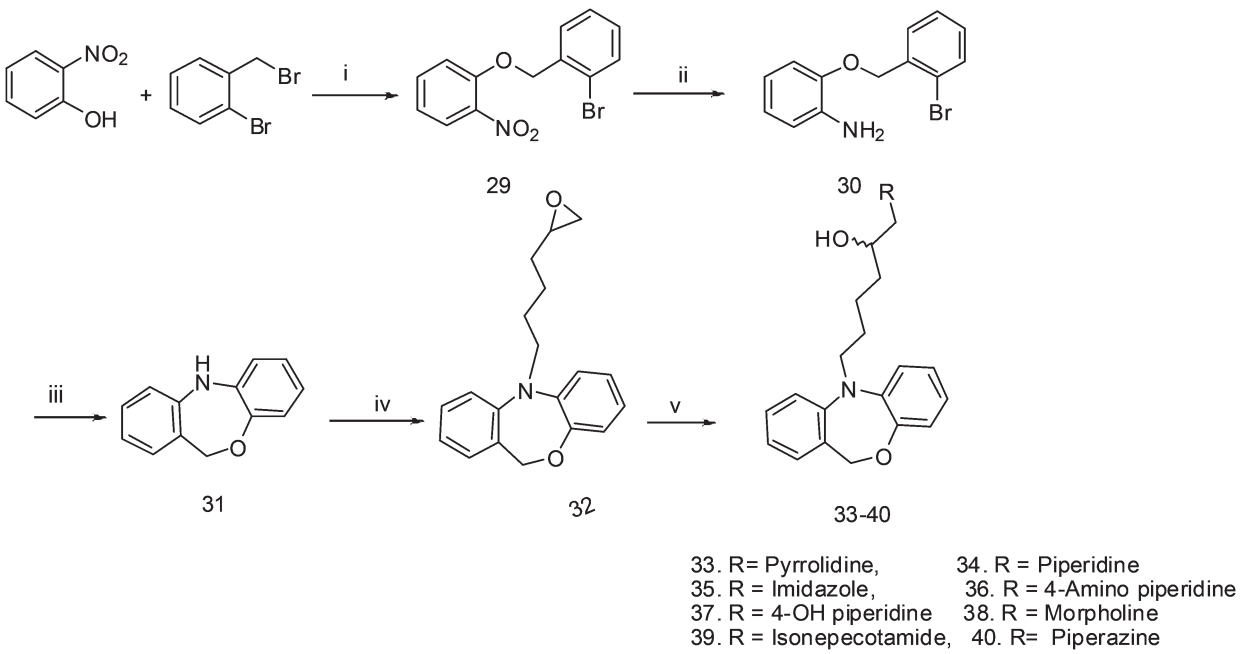

Scheme 2 Synthesis of prototype II compounds. Reagents and conditions: (i) K_2CO_3, dry acetone, reflux, 3 h, 95%; (ii) Fe/HCl, EtOH, reflux 4–5 h, 78%; (iii) CuI, L-proline, *t*-BuOK, DMF, N_2, 110 °C, 24 h, 50%; (iv)) NaH, 4, dry DMF, 0 °C-RT, 1 h, 85%; (v) 2° amine, EtOH, reflux, 12 h, 68–75%.

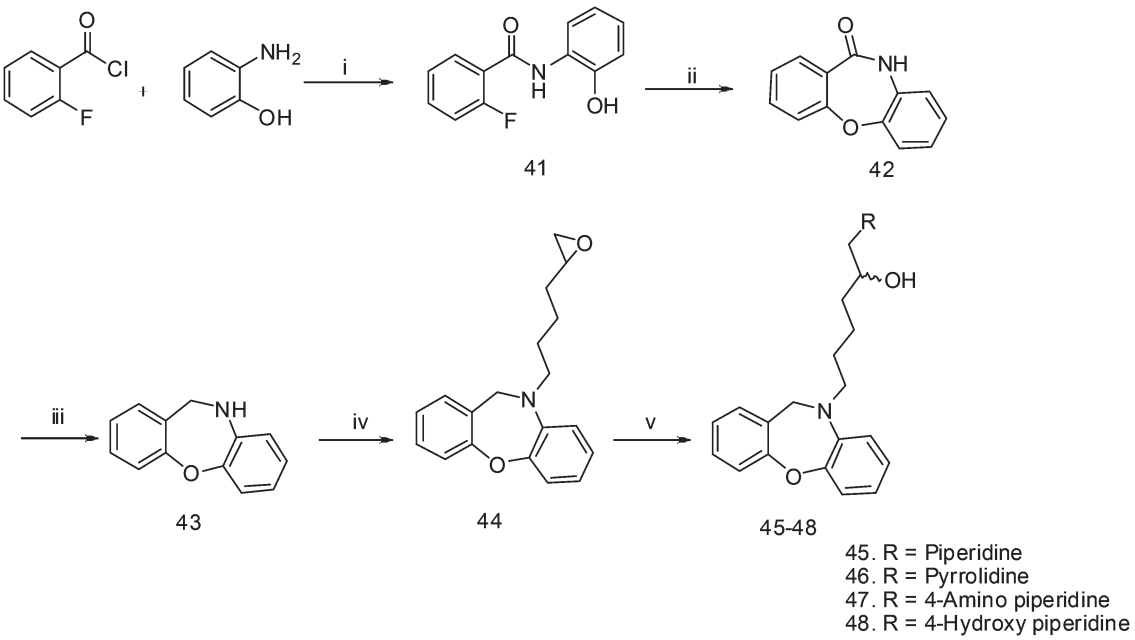

Scheme 3 Synthesis of rototype III compounds. Reagents and conditions; (i) Et_3N, THF, 0 °C-RT, 12 h, 74%; (ii) NaOH, DMF, 120 °C, 5 h, 78%; (iii) $LiAlH_4$, THF, 70 °C, 85%; (iv) NaH, 4, dry DMF, 0 °C-RT, 1 h, 88%; (v) 2° amine, EtOH, reflux, 12 h, 70–75%.

In silico docking calculations

Controlled docking studies using the AMP structure already present in the crystal structure and Autodock 3.0.5 were performed as described earlier.[39] The reference molecule, AMP, adopted a similar conformation as reported in the crystal structure (Fig. 1A), validating the computational strategy. The conformations of the docked inhibitors were observed to be similar to the conformation of the AMP moiety, occupying the same binding site (Fig. 1B). After the AutoDock simulations were complete, the binding energy of the docked inhibitor structures were analyzed (Table 1). Docking energy scores ranging from −12.9 to −10.6 kcal mol^{-1} were obtained, suggesting that the tested compounds might be the inhibitors of the enzyme.

Hydrogen bonding parameters between the DNA ligase and the inhibitors were visualized using PyMOL (v.1.2r3pre; Schrodinger LLC). The analysis highlighted some key residues that were consistently participating in the binding of all the inhibitors. Interactions for control AMP was also compared (Fig. 1A). Leu90, Ser91, Leu92, Asn94, Glu121, Leu122, Lys123, Ala124, Ala128, Arg144, Arg182, Glu184, His236, Val298 and Lys300 were predicted to form hydrogen-bonding interactions with the compounds. Lys123, an essential residue, shows polar interactions with all the compounds that show good inhibition. The stacking interactions of the compounds with His236 appeared to be a characteristic feature of compound recognition in MtbLigA.

In vivo/antibacterial assays

Two bacterial systems were employed in order to evaluate the *in vivo* inhibition of NAD^+ ligases, as previously reported.[35,40] The first system used in the assays was a temperature sensitive *E. coli* GR501 strain that carries a *lig251* mutation in its LigA gene, due to which it grows normally at 30 °C. However, its growth is strongly hampered at physiological temperatures. This deficiency is overcome by complementing it with NAD^+ or ATP dependent ligases.[41–43] Consequently, this strain has been used to study the *in vivo* specificity of inhibitors for LigA. We also used pTrc99A-based systems, involving MtbLigA and T4Lig in this strain.[44]

Next, to test whether the compounds also act upon NAD^+ ligases from other bacterial sources, a well-known human pathogen, *S. typhimurium*, LT2 strain was used.[45] Its DNA ligase null derivative, TT15151 has been salvaged by T4 DNA ligase.[46] These two independent bacterial systems allowed us to explore the *in vivo* inhibition of LigA and ATP-dependent ligases by the given compounds.

E. coli GR501 strain, possessing only the pTrc99A plasmid, demonstrated high sensitivity to the compounds (Table 2) compared to the corresponding ligase-complemented strains due to the remnant ligase activity in the mutant strain relative to the growth-rescued strains, which harbour a high copy number of the overexpressed ligase used to retrieve them. This is similar to the observations in the case of pyridochromanones, glycosyl ureides, glycosyl amines, and cycloalkanones.[35,40,41] The results obtained after bactericidal studies done for the compounds demarcated eight compounds to be potentially active with low MIC values out of thirty five indole derivatives that were tested against MtbLigA. These eight compounds (Table 2) had ~1.5–3-fold lower MICs for the strain rescued by MtbLigA than for the strain rescued by T4 ligase. A similar trend was also observed in the case of *S. typhimurium*

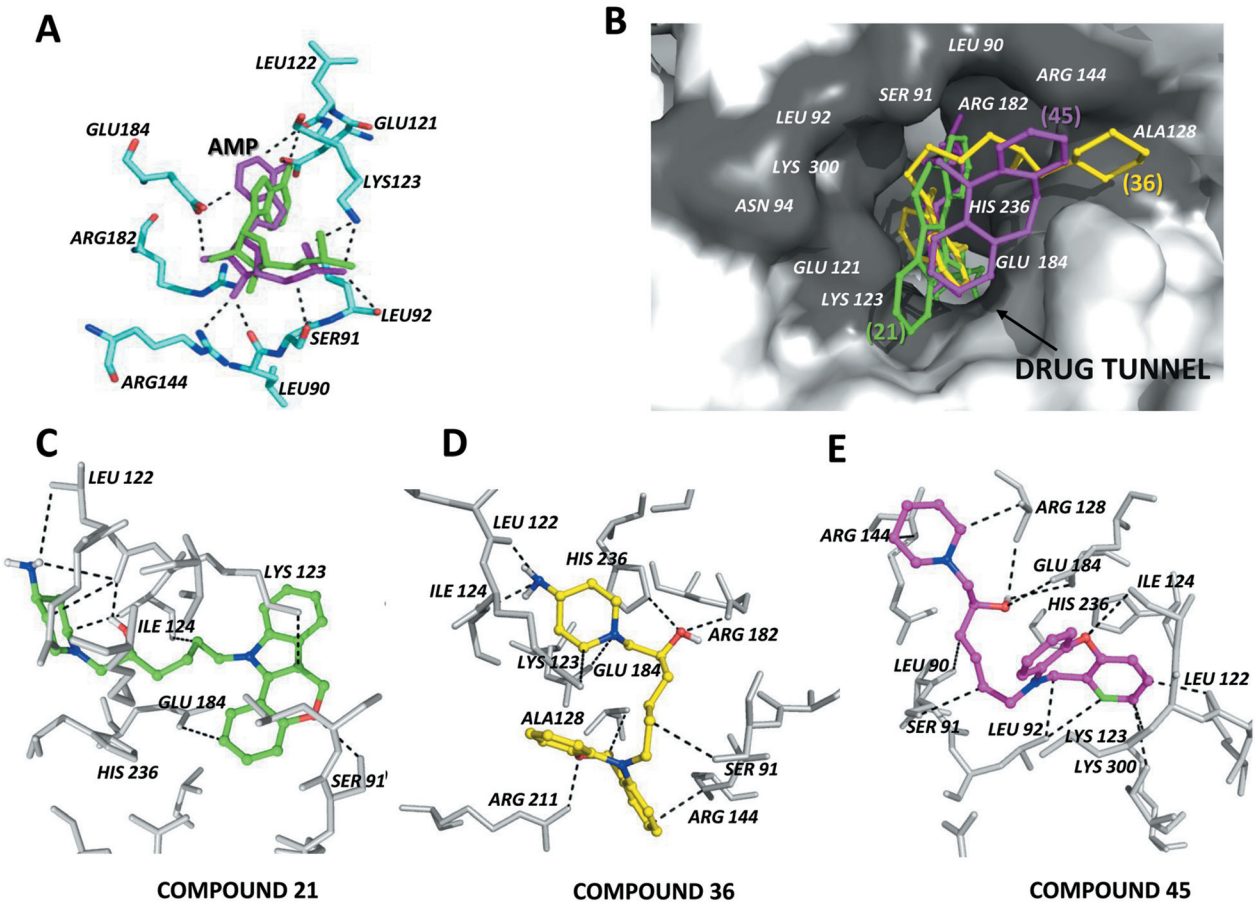

Fig. 1 Docking analysis: (A) docking of AMP in the catalytic site. AMP in the crystal structure (green sticks) and docked AMP (magenta sticks) exhibit similar conformations. Active site residues are depicted as balls-and-sticks and are labeled in black. Hydrogen bonds are shown as dashed lines. (B) Surface representation of DNA Ligase showing inhibitor **21** (pale Green), **36** (yellow) and **45** (magenta) sticks docked into the binding cleft of the protein. The protein has surface representation shown in white and dark grey denotes the substrate binding cleft. (C) Docked confirmations of inhibitor **21** (pale green stick) at the binding cleft. (D) Docked confirmations of inhibitor **36** (yellow stick) at the binding cleft. (E) Docked confirmations of inhibitor **45** (magenta stick) at the binding cleft. Active site residues are depicted as balls-and-sticks and are labeled in black. Bond interactions are shown in dashed lines.

Table 1 *In vitro* inhibition of MtbLigA (NAD^+ dependent), T4 DNA ligase, and human DNA ligase I (ATP-dependent) by the respective compounds and their docking energies

		$IC_{50}(\mu M)$			
S. No	Compound no	MtbLigA[a]	T4Lig	HuLigI	Docking energies[b] (kcal mol^{-1})
1	**17**	>100	>240	285 ± 6	−12.5
2	**21**	65 ± 5	110 ± 8	274 ± 9	−12.9
3	**36**	70 ± 3	110 ± 6	245 ± 6	−12.3
4	**39**	>200	>300	ND[c]	−12.6
5	**40**	200	>300	ND	−11.0
6	**45**	35.2 ± 3	150 ± 10	282 ± 6	−12.1
7	**46**	>100	>250	278 ± 5	−10.6
8	**48**	>200	>300	ND	−12.4

[a] Mtb, *M. tuberculosis*. [b] Docking energies were calculated for respective compounds and Mtb NAD^+-dependent DNA ligase by Autodock 3.0.5 as described in Methods [c] ND, not determined.

(Table 2). As revealed by the time kill studies, these compounds exhibited more sensitivity to the *S. typhimurium* wild-type LT2 strain harbouring the NAD^+ dependent ligase compared to its ligase-deficient mutant TT1515, rescued by ATP-dependent ligase (Fig. 2 and S1†). The lower potency of inhibitors against ATP ligase rescued strains signifies that the inhibitory effect of the compounds is unlikely to be an off-target effect. The *in vivo* bactericidal studies aided us to screen potential compounds that could discriminate between NAD^+ and ATP dependent DNA ligases for further *in vitro* analysis.

In vitro enzymatic assays

To rapidly assess the potential of the synthesised compounds as specific inhibitors of MtbLigA, we performed assays wherein the eight indole/dihydrobenzoxepine compounds with low MICs, demarcated by bactericidal assays, were examined at elevated concentrations (150 μM) against purified MtbLigA, T4 ligase and human DNA ligase I in respective ligation assays.

Table 2 Antibacterial activity of the tricyclic dihydrobenzoxazepine and tetracyclic indole derivatives

MIC[a]						
Compound no.	Compound's structure	*E. coli* GR501+ *pTrc99A*	*E. coli* GR 501+ Mtb NAD^+ ligase	*E. coli* GR501+ T4 DNA ligase	*S. typhimurium* LT2	*S. typhimurium* TT15151
17	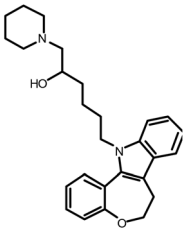	0.4	15	25	30	>100
21	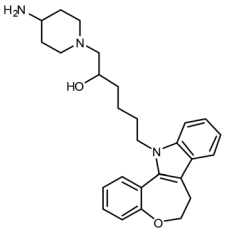	0.4	10	40	20	50
36	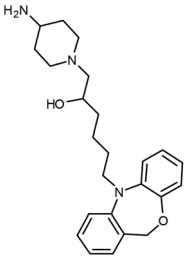	0.4	12	24	15	20
39	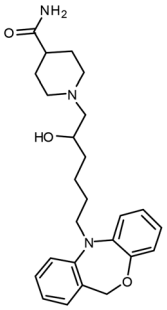	0.6	16	60	12	25
40	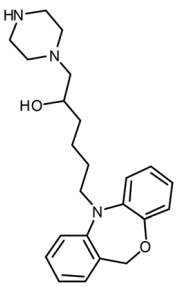	0.4	10	30	10	12
45	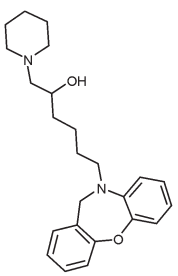	0.6	16	24	16	32

Table 2 *(Contd.)*

MIC[a]						
Compound no.	Compound's structure	*E. coli* GR501+ *pTrc99A*	*E. coli* GR 501+ Mtb NAD^+ ligase	*E. coli* GR501+ T4 DNA ligase	*S. typhimurium* LT2	*S. typhimurium* TT15151
46	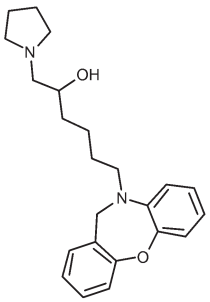	0.5	12	20	12	32
48	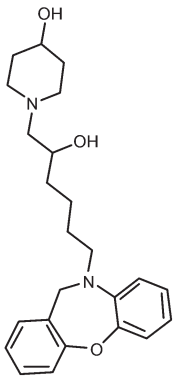	0.5	10	60	15	21

[a] The MIC values are given in μg ml^{-1}. The strains used in the study are explained in the text. All compounds except for the ones listed in the table were tested from 0–200 μg ml^{-1} concentration but they did not show any inhibitory activity.

Potential compounds that could discriminate between NAD^+ and ATP-dependent DNA ligases were thus identified for further analysis. Of the eight indole/dihydrobenzoxepine derivatives, compounds with $-NH_2$ groups at R_1 position and –OH at R_2 position were able to distinguish better between two classes of enzymes by a factor of around 2. The results are summarized in Table 1. Although the cyclic indole/dihydrobenzoxepine derived compounds inhibited MtbLigA with lesser IC_{50} values, the human DNA ligase I was much less sensitive to the compounds and was inhibited with IC_{50} values higher than 250 μM, as shown in the Table 1.

In silico docking analysis suggested an overlap of the binding sites of NAD^+ and the synthesised indole and dihydrobenzoxazepine derivatives. We, therefore, chose the best compounds, **21**, **36** and **45**, for standard kinetics analysis to explore their competitive action with respect to NAD^+ in *in vitro* nick sealing assays. In the absence of the inhibitor, we determined a K_m of 1.7 ± 0.2 μM for NAD^+ in the presence of 10% Me_2SO in the reaction mixture, which was in agreement with previously reported data.[35,40,47] The analysis of the nick sealing assays in the presence of different concentrations of compounds **21**, **36** (0–250 μM) and **45** (0–100 μM) with increasing concentration of NAD^+ (0–60 μM) clearly indicated a competitive inhibition of NAD^+ by compounds, also revealed by their double reciprocal plots (Fig. S2, S3† and Fig. 3, respectively). The linear regression using the apparent K_m values lead to a K_i of 97.7 μM for compound **21** (Fig. S1†), 94.2 μM and 56.6 μM for compounds **36** and **45**, respectively (Fig. S2 and 3,† respectively). These results clearly suggest that the binding sites of the cyclic indoles/dihydrobenzoxazepines overlaps with NAD^+. Although all the three compounds, **21**, **36**, and **45**, showed a competitive mode of inhibition, compound **45** stands out as a potentially strong inhibitor of MtbLigA with significantly lower K_i value. This result is in agreement with the docking analysis, which showed that compound **45** makes the largest number of hydrogen bonds/polar and hydrophobic interactions with the essential residues lining the cofactor binding site. The tricyclic dihydrobenzoxazepines (**36** and **45**) also interact well with the NAD^+ binding site. The –OH at R_2 position of **45** is involved in donor/acceptor interactions with the catalytic residue Glu184, while stacking interactions is seen between the aromatic rings of the compound and His236 (Fig. 1E). The compound is also well positioned to exhibit interactions with critical residues like Lys300, Ser91, and Arg 144. However, the introduction of $-NH_2$ group at position R_1 in compound **36** (Fig. 1C) results in the loss of important interactions with the critical Lys 300 and Leu90 and might result in lower potency of the compound compared to **45**. The compound **21**

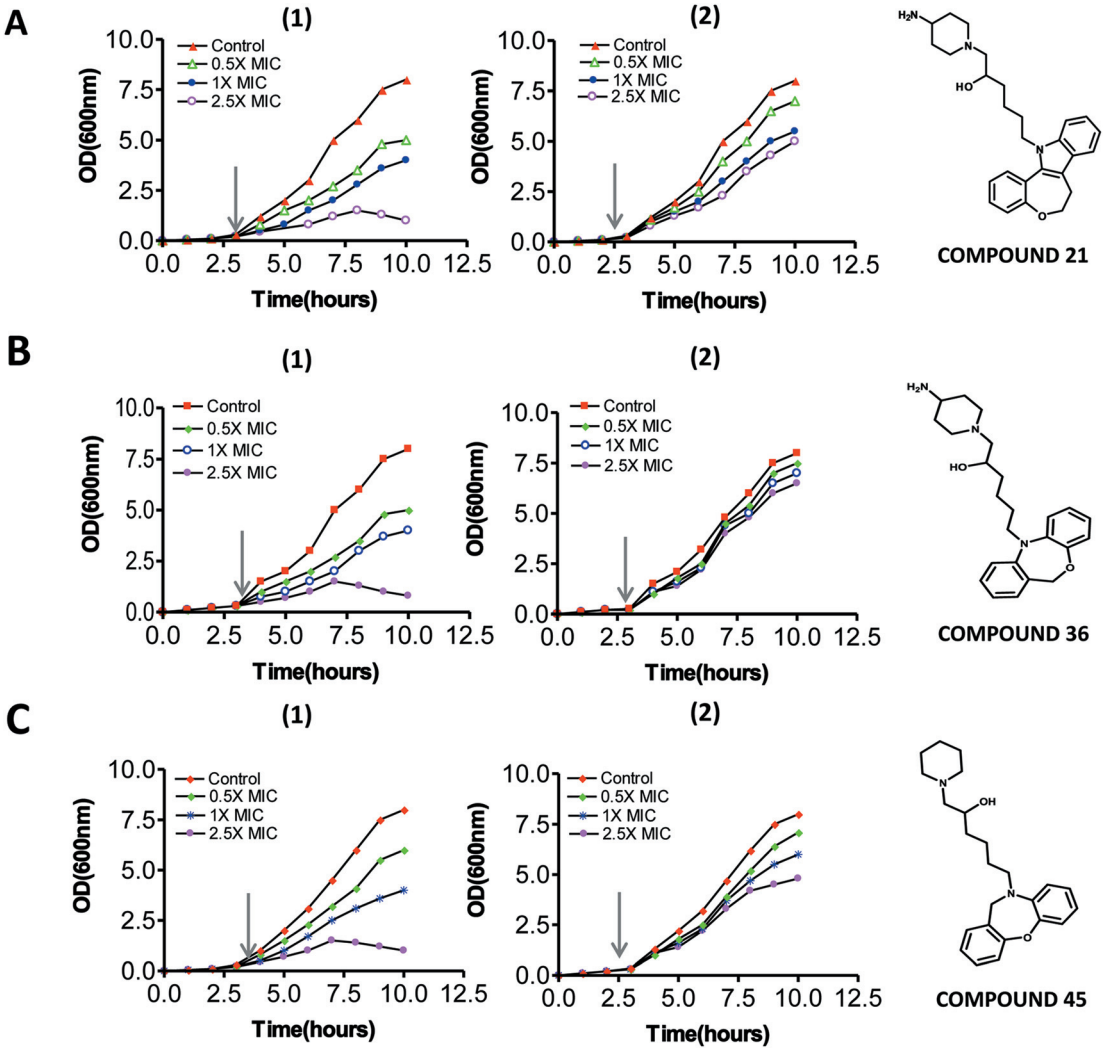

Fig. 2 Bactericidal activity of compounds (A) **21** (B) **36** (C) **45**. Effect on growth as reflected in changes of the optical density at 600 nm of (1) *S. typhimurium* LT2 and (2) its DNA ligase minus (null) derivative TT15151 [Lig^{-}/T4 Lig^{+}] on their respective exposures to compounds in μg ml^{-1} representing 0.5 to 2.5 times the MIC value. The arrow indicates the point at which the compound was added. The structures of the respective compounds are shown beside the graphical representation of the experiments.

(Fig. 1D) with bulky tetracyclic structure makes favourable interactions with few of the critical residues, which make it active in our assays but it lacks important interactions with Lys300, Arg 144 and Leu 90, making it less potent than **45**.

DNA–inhibitor interaction assays

We performed ethidium bromide displacement assays for the selected inhibitors in the current study to assess their interactions with DNA, if any. It was earlier reported that aryl amino compounds, a class of DNA ligase inhibitors, generally intercalate with DNA, which might affect their inhibitory potencies.[48] A maximum concentration of 250 μM (50 times of EtBr) of the respective compounds **21**, **36** and **45** was added to the reaction mixture containing EtBr-DNA and analysed by fluorescence spectra. We did not observe any marked displacement of ethidium bromide even at the highest concentration of the compounds (Fig. S4A, B, C†).

Gel shift assays were also performed to probe for any general inhibitor–DNA interactions in the presence of increasing concentration of inhibitors. The results did not show any shift in the position of the DNA bands with increasing compound concentration and clearly suggest that the cyclic indoles do not exhibit any general interactions with DNA (Fig. S4D†).

Methods

In silico screening and docking

All the synthesized ligase inhibitors (Fig. 1) were constructed by full energy minimization using the BUILDER module in

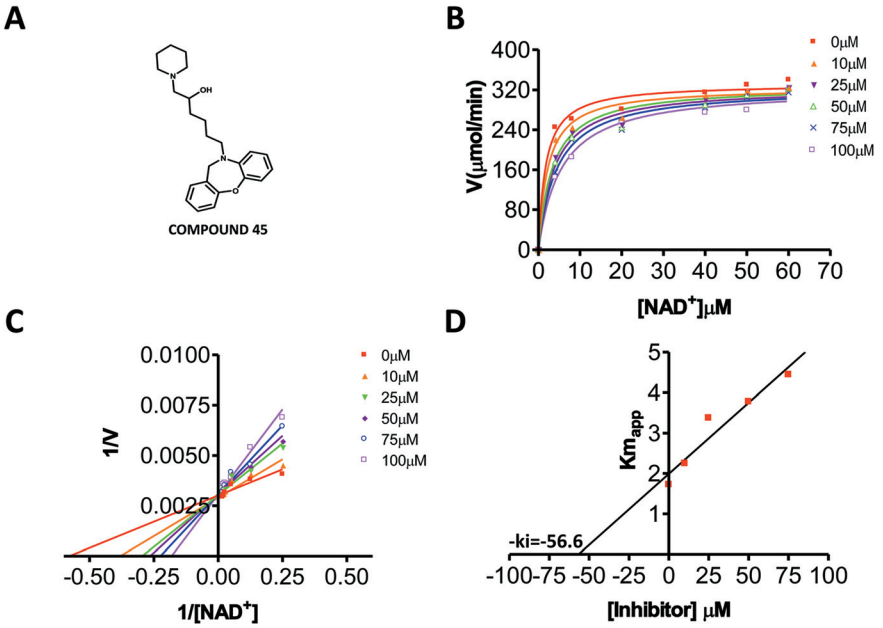

Fig. 3 Competitive inhibition of MtbLigA with respect to NAD^+ by the compound **45**. (A) Structure of compound **45**. (B) Activity of MtbLigA measured in the presence of rising concentrations of compound **45** (0–100 μM) and NAD^+ (0–50 μM). (C) The double reciprocal plot shows competitive binding between NAD^+ and compound **45**. (D) K_i value for the compound **45** was calculated to be 56.6 μM.

Insight II software (ver. 2000.1 Accelrys Inc.). The crystal structure of the adenylation domain of MtbLigA (PDB ID: 1ZAU) was used for docking after being shorn of the water molecules and heteroatoms. The binding pocket of DNA ligase is bordered by the residues Leu90, Ser91, Asn94, Glu121, Leu122, Lys123, Ala124, Arg144 and Glu184. The docking studies were carried out using the Autodock 3.0.5.[49] The Kollman charges, solvation parameters and polar hydrogens were added and the charges on residues were neutralized. The ligands were prepared for calculations by adding gasteiger charges. The cubic grid box size was set at 64 Å × 54 Å × 58 Å (x, y, and z) with spacing of 0.375 Å, which included all the amino acid residues that were present in the catalytic site. AutoGrid 8 program was used to produce grid maps. The rest of the parameters were set to the standard default values. The population size was set to 150 and the individuals were initialized randomly. A maximum of 20 poses were evaluated for each compound using the Lamarckian genetic algorithm (LGA) with the medium number of energy evaluations (250 000). The Autodock results were analyzed to study the interactions and the binding energy of the respective docked structures.

Antibacterial activity and inhibition of ligase *in vivo*

Two specific ligase deficient (*E. coli* and *S. typhimurium*) bacterial strains were employed to study the effect of inhibitors on their growth. The recombinant plasmid pRBL[44] carrying the gene for T4Lig in pTrc99A was transformed into temperature sensitive *E. coli* GR501 $ligA^{ts}$ mutant.[42] The MtbLigA clone in pTrc99A was also transformed into *E. coli* GR501 so as to have the same genetic background.[40] The growth of strains expressing MtbLigA or T4Lig were compared with a control GR501 strain carrying empty pTrc99A without any gene insertions at 37 °C. As reported earlier[41] and reproduced by us, the temperature-sensitive *E. coli* GR501 $ligA^{ts}$ strain grows well at 30 °C, while the robust impediment of growth occurs at 37 °C. Complementation with either MtbLigA or T4Lig re-establishes the growth of the mutant strain.

As another system for investigating the specificity of inhibitors *in vivo* and to monitor their action against other NAD^+-dependent DNA ligases, we used *S. typhimurium* wild type LT2 strain and its DNA ligase deficient null derivative TT1515, which had been salvaged with a plasmid (pBR313/598/8/1b) encoding T4 ligase gene.[46] Minimum inhibitory concentrations (MICs) of the inhibitors were determined for both the abovementioned bacterial strains. The MIC values were determined in broth microdilution assays in microtiter plates in a volume of 200 μL. Serial 2-fold dilutions of antibacterial compounds were seeded with inoculums containing approximately 10^5 colony-forming units per ml in the case of *E. coli* $ligA^{ts}$ mutant and 10^6 colony-forming units per ml in the case of *S. typhimurium* LT2 and its $LigA^-$ mutant strain, rescued with T4 DNA ligase, under ambient conditions for 20 h. The MICs were inferred as the lowest concentrations of compounds that prevented visible microbial growth. *E. coli* mutant strain was grown in LB medium, whereas the *S. typhimurium* strains were grown in nutrient broth. In the case of *E. coli*, the medium contained 25 μg ml^{-1} polymyxin B nonapeptide (Sigma-Aldrich) to facilitate penetration of the inhibitors across the outer membrane.

Time-kill studies

An exponentially growing culture of *S. typhimurium* LT2 and its DNA ligase-null mutant derivative in nutrient broth were treated at A_{600} = 0.4 with increasing inhibitor concentrations. The effect on growth and viability was investigated by monitoring the A_{600} and the number of CFU for 6–7 hours following the addition of the antibacterial compound. For quantification of the CFU, culture aliquots of both the strains were serially diluted in phosphate-buffered saline and plated on a nutrient agar. After incubation for 16 h at 37 °C, colonies were visible on the plate.

In vitro enzyme inhibition assays

DNA substrate used for performing the *in vitro* ligation activity assays was a 40 base pair duplex DNA containing a single stranded nick between bases 22 and 23, as reported earlier.[17,34,35] Briefly, the substrate was generated using three oligonucleotides that were annealed in Tris/EDTA buffer: *viz.*, a 40 nucleotides long template oligomer (5′-ATG TCC AGT GAT CCA GCT AAG GTA CGA GTC TAT GTC CAG G-3′), to 18 nucleotides 5′ 6-FAM labelled (5′-AGC TGG ATC ACT GGA CAT-3′) and 22 nucleotides (5′-CCT GGA CAT AGA CTC GTA CCT T-3′). This fluorescently labelled nicked 40 base-pair duplex DNA substrate was employed to investigate the *in vitro* inhibitory activity of diverse compounds against MtbLigA, bacteriophage T4Lig and human DNA ligase I. The quantities of the individual enzymes were optimized for comparable degree of ligation, lacking any inhibitor under the assay conditions.[50]

Full-length MtbLigA was expressed and purified as earlier.[40] The assays were carried out using 2 ng of the purified protein. A standard ligation assay reaction mixture (20 μl) contained 50 mM Tris-HCl (pH 8.0), 10 mM $MgCl_2$, 5 mM DTT, 10% dimethyl sulfoxide (Me_2SO), 2 μM NAD^+ and 2 pmol FAM labelled nicked duplex DNA substrate and different concentration of the compounds. The reactions were assembled on ice, incubated at 25 °C for 60 minutes. The termination of reactions was done by adding 10 μl of the stop solution (98% formamide, 10 mM EDTA, 0.15% xylene cyanol and 0.15% bromophenol blue). Samples were heated for 5 minutes at 100 °C and chilled on ice before loading. The reaction products were resolved on 15% polyacrylamide gels containing 8 M urea 90 mM Tris borate and 2.5 mM EDTA. Gels were scanned using Image Quant LAS 4000 (M per s GE healthcare) and band intensities of the ligated product were measured and quantified using the ImageQuantTL 8.1 software. Since all the compounds were soluble in 100% $(CH_3)_2SO$ and encompassed one-tenth volume of the ligation reaction mixture, the control reaction too included 10% $(CH_3)_2SO$.

T4 DNA ligase assay was performed in reaction mixture containing 0.05 U of enzyme (Amersham), 2 pmol of labelled template and 66 μM ATP in 66 mM Tris–HCl, pH 7.6 mM $MgCl_2$, 10 mM DTT and 10% Me_2SO. The expression plasmid of Human DNA ligase I was transformed into *E. coli* BL21 (DE3) and the protein was purified as illustrated previously.[50] The procedure used to carry out the ligation assay was same as described above. 2 μg protein was used in 50 mM Tris–HCl, pH 8.0, 10 mM $MgCl_2$, 5 mM DTT, 50 mg ml^{-1} BSA and 1 mM ATP.

Calculation of IC_{50} values

The potency of the compounds was measured by determining its IC_{50} values by adding appropriate concentrations of the compound to the reaction mixture prior to the addition of the substrate in *in vitro* ligation assays. The IC_{50} values were determined by plotting the relative ligation activity *versus* inhibitor concentration and fitting to the equation: $V_i/V_0 = IC_{50}/(IC_{50} + [I])$ using the GraphPad Prism software. V_0 and V_i correspond to the rates of ligation in the absence and presence of inhibitor, respectively, and [I] represent the inhibitor concentration.

Mode of inhibition

The saturating substrate concentration for MtbLigA was determined by increasing the NAD^+ concentration from 0 μM to 60 μM, employing Michaelis–Menten kinetics. K_m for NAD^+ was determined in 10% $(CH_3)_2SO$ using the above described assay procedure. The kinetics for different amounts of compounds were determined using varying concentrations of NAD^+ under standard assay conditions as described earlier.[35]

The rate of the ligation reaction was determined based on the extents of ligation by scanning the gel using Image Quant LAS 4000. The data was plotted using Michaelis–Menten kinetics in Graph Pad Prism, where the abscissa denoted NAD^+ concentration and ordinate corresponded to the rate of ligation. Likewise, K_i values were determined by plotting the apparent K_m values against the respective compound concentrations. The mode of inhibition was determined through the standard analysis of Lineweaver–Burk kinetics.

DNA–inhibitor interactions

Ethidium bromide displacement assay. The intercalating properties of the antibacterial compounds were monitored by its ability to displace ethidium bromide from DNA by competing with it for DNA binding. The displacement of ethidium bromide from DNA was measured by monitoring the loss in the fluorescence, occurring due to its detachment from the duplex DNA.[51] The reaction mixture contained 5 μg of calf thymus DNA, 5 μM ethidium bromide, 25 mM Tris-HCl (pH 8.0), 50 mM NaCl, and 1 mM EDTA in total volume of 100 μl. The fluorescence analysis of ethidium bromide was instantly done at an excitation wavelength of 485 nm and emission wavelength of 612 nm using a Perkin Elmer spectrofluorometer LS55.

Gel shift assay. Gel shift assays were performed using 100 ng of plasmid DNA (pUC18, Stratagene) incubated with increasing concentrations of inhibitors in TE buffer for 1 hour at room temperature. Subsequently, DNA shift was analysed on a 1.5% agarose gel.

Conclusions

The present study was undertaken to probe for the specific inhibitory action of the tetracyclic indole and tricyclic dihydro-

benzooxazepine derivatives against MtbLigA. Overall, the studies revealed that tetracyclic and tricyclic indole derivatives could distinguish between the two classes of ligases. The *in vivo* studies support that the possible mode of action of the compounds are due to inhibition of the essential LigA in bacteria. The compounds also did not display general interactions with DNA and act by competing with the cofactor NAD^+. The ongoing focus is the development of next generation derivatives that exhibit improved potency and specificity for LigA. Being smaller in size, these molecules are suitable for further optimisation.

Experimental section

General procedure for the synthesis of target molecules

The respective epoxy compounds and dry secondary amines (1.2 eq.) were dissolved in absolute ethanol (5–10 ml) and the solutions were refluxed under continuous stirring for 10–12 h. After completion of the reaction, ethanol was removed under vacuum to give the crude products as coloured oily liquids. The crude compounds were purified by column chromatography using neutral alumina as adsorbent and MeOH/$CHCl_3$ as eluent to afford the pure products.

6-(6,7-Dihydro-12*H*-benzo[2,3]oxepino[4,5-*b*]indol-12-yl)-1-(piperidin-1-yl)hexan-2-ol (17). Colourless viscous liquid (150 mg, 72%). ^{1}H NMR (300 MHz, $CDCl_3$) δ 7.61–7.58 (d, J = 7.6 Hz, 1H), 7.48–7.42 (m, 2H), 7.30–7.19 (m, 5H), 4.63–4.59 (t, J = 6.4 Hz, 2H), 4.33–4.28 (t, J = 7.3 Hz, 2H), 3.65–3.62 (m, 1H), 3.39 (brs, 2H), 3.08–3.04 (t, J = 6.4 Hz, 2H), 2.67–2.66 (m, 2H), 2.27–2.25 (d, J = 6.5 Hz, 2H), 2.08–203 (m, 3H), 1.83–1.80 (m, 5H), 1.78–1.65 (m, 4H). ^{13}C NMR (50 MHz, $CDCl_3$) δ 142.3, 139.4, 137.3, 136.3, 133.0, 130.1, 127.9, 127.7, 127.3, 126.3, 121.6, 119.4, 118.3, 114.8, 114.3, 110.3, 67.7, 62.1, 54.4, 43.9, 34.6, 34.0, 33.0, 32.1, 29.6, 29.4, 29.2, 23.6, 22.9, 22.8. IR (neat, cm^{-1}): 3401, 3019, 2941, 2399, 1606, 1384, 1215, 1083, 757, 669. ESI-MS: (m/z) = 419 $[M + H]^+$. HRMS (ESI) exact mass calcd for $[C_{27}H_{34}N_2O_2 + H]^+$ 419.2620, found 419.2704.

1-(4-Aminopiperidin-1-yl)-6-(6,7-dihydro-12*H*-benzo[2,3]-oxepino[4,5-*b*]indol-12-yl)hexan-2-ol (21). Light yellow viscous liquid (152 mg, 70% yield). ^{1}H NMR (300 MHz, $CDCl_3$) δ 7.60–7.58 (d, J = 7.8 Hz, 1H), 7.47–41 (m, 2H), 7.31–7.14 (m, 5H), 4.62–4.58 (t, J = 6.4 Hz, 2H), 4.31–4.26 (t, J = 7.5 Hz, 2H), 3.08–3.03 (t, J = 7.2 Hz, 2H), 2.93–2.89 (m, 4H), 2.73.2.69 (m, 3H), 2.39–2.27 (m, 4H), 2.18–1.98 (m, 3H), 1.43–1.39 (m, 4H). ^{13}C NMR (50 MHz, $CDCl_3$) δ 157.2, 138.0, 128.3, 127.4, 126.9, 123.8, 123.1, 121.9, 119.5, 118.1, 114.0, 112.9, 110.3, 66.1, 63.9, 54.0, 51.0, 48.5, 44.5, 35.8, 34.3, 29.9, 29.7, 24.4, 22.8. IR (neat, cm^{-1}): 3401, 3019, 2929, 1644, 1384, 1215, 1084, 758, 669. ESI-MS: (m/z) = 434 $[M + H]^+$. HRMS (ESI) exact mass calcd for $[C_{27}H_{35}N_3O_2 + H]^+$ 435.2841, found 435.2645.

1-(4-Aminopiperidin-1-yl)-6-(dibenzo[*b*,*e*][1,4]oxazepin-5-(11*H*)-yl)hexan-2-ol (36). Colourless viscous liquid (135 mg, 68%). ^{1}H NMR (300 MHz, $CDCl_3$) δ 7.31–7.28 (m, 2H), 7.11–6.69 (m, 3H), 6.84–6.79 (m, 3H), 5.31(s, 2H), 3.77–3.73 (t, J = 6.6 Hz, 2H), 3.59–3.56 (m, 1H), 2.93–2.68 (m, 3H), 2.22–2.18 (m, 5H), 1.81–1.66 (m, 4H), 1.40–1.27 (m, 5H). ^{13}C NMR (50 MHz, $CDCl_3$) δ150.9, 149.4, 136.1, 132.0, 129.3, 128.7, 123.0, 122.4, 121.1, 120.6, 119.8, 119.5, 69.8, 67.1, 65.8, 64.7, 53.7, 50.3, 34.4, 29.8, 27.7, 23.2. IR (neat, cm^{-1}): 3400, 3019, 2928, 2399, 1602, 1489, 1384, 1215, 1084, 928, 757, 669. ESI-MS: (m/z) = 396 $[M + H]^+$. HRMS (ESI) exact mass calcd for $[C_{24}H_{34}N_3O_2 + H]^+$ 396.2651, found 396.2573.

1-(6-(Dibenzo[*b*,*e*][1,4]oxazepin-5(11*H*)-yl)-2-hydroxyhexyl)-piperidine-4-carboxamide (39). Light yellow viscous liquid (160 mg, 75%). ^{1}H NMR (300 MHz, $CDCl_3$) δ 7.31–7.28 (m, 2H), 7.11–6.99 (m, 3H), 6.80–6.78 (m, 3H), 5.79 (s, 1H), 5.57 (s, 1H), 5.31 (s, 2H), 3.77–3.73 (t, J = 6.6 Hz, 2H), 3.61–360 (m, 1H), 3.02–2.99 (m, 1H), 2.79–2.15 (m, 4H), 1.91–1.83 (m, 4H), 1.79–1.74 (m, 4H), 1.70–1.66 (m, 4H). ^{13}C NMR (50 MHz, $CDCl_3$) δ 177.7, 150.8, 149.3, 136.0, 131.9, 129.2, 128.6, 122.8, 122.3, 121.0, 120.5, 119.7, 119.3, 114.1, 69.7, 66.1, 64.2, 54.8, 51.5, 50.2, 42.5, 34.4, 33.8, 31.9, 31.6, 29.7, 29.5, 28.9, 27.6, 23.1, 22.7. IR (neat, cm^{-1}): 3408, 3020, 2930, 2401, 1675, 1599, 1489, 1262, 1076, 928, 760, 670. ESI-MS: (m/z) = 424 $[M + H]^+$. HRMS (ESI) exact mass calcd for $[C_{25}H_{34}N_3O_3 + H]^+$ 424.2600, found 424.2618.

6-(Dibenzo[*b*,*e*][1,4]oxazepin-5(11*H*)-yl)-1-(piperazin-1-yl)-hexan-2-ol (40). Colourless viscous liquid (130 mg, 69%). ^{1}H NMR (300 MHz, $CDCl_3$) δ 7.12–7.02 (m, 2H), 6.80–6.59 (m, 3H), 6.54–6.50 (m, 3H), 5.32 (s, 2H), 3.76–3.72 (t, J = 6.5 Hz, 2H), 3.62 (s, 1H), 3.13–2.61 (m, 4H), 2.59–2.50 (m, 2H), 2.30–2.18 (m, 5H), 1.69–1.38 (m, 5H). ^{13}C NMR (50 MHz, $CDCl_3$) δ 150.8, 149.2, 135.9, 131.9, 129.2, 128.6, 122.8, 122.2, 120.9, 120.5, 119.6, 119.3, 69.6, 65.7, 64.7, 54.3, 50.23, 46.1, 34.4, 27.6, 23.1. IR (neat, cm^{-1}): 3401, 3019, 2399, 1602, 1384, 1215, 1084, 928, 758, 669. ESI-MS: (m/z) = 382 $[M + H]^+$. HRMS (ESI) exact mass calcd for $[C_{23}H_{32}N_3O_2 + H]^+$ 382.2495, found 382.2497.

6-(Dibenzo[*b*,*f*][1,4]oxazepin-10(11*H*)-yl)-1-(piperidin-1-yl)-hexan-2-ol (45). Light yellow viscous liquid (130 mg, 68%). ^{1}H NMR (300 MHz, $CDCl_3$) δ 7.18–7.15 (m, 1H), 7.12–7.05 (m, 4H), 6.95–6.83 (m, 1H), 6.81–6.76 (m, 2H), 4.41 (s, 2H), 3.69 (s, 1H), 3.22–3.17 (t, J = 7.2 Hz, 2H), 2.64–2.63 (m, 2H), 2.35–2.25 (m, 3H), 2.21–1.72 (m, 5H), 1.65–1.43 (m, 8H). ^{13}C NMR (50 MHz, $CDCl_3$) δ 157.8, 148.1, 141.5, 130.4, 128.7, 128.3, 124.4, 123.6, 120.1, 65.6, 64.6, 54.8, 53.1, 34.8, 29.6, 27.9, 25.0, 23.6, 23.1. IR (neat, cm^{-1}): 3401, 3019, 2928, 2399, 1601, 1384, 1215, 1084, 928, 758, 627. ESI-MS: (m/z) = 381 $[M + H]^+$. HRMS (ESI) exact mass calcd for $[C_{24}H_{33}N_2O_2 + H]^+$ 381.2542, found 381.2543.

6-(Dibenzo[*b*,*f*][1,4]oxazepin-10(11*H*)-yl)-1-(pyrrolidin-1-yl)-hexan-2-ol (46). Light yellow viscous liquid (130 mg, 71%). ^{1}H NMR (300 MHz, $CDCl_3$) δ 7.25–7.10 (m, 5H), 7.08–7.05 (m, 1H), 6.96–6.76 (m, 2H), 4.41 (s, 2H), 3.2 (s, 1H), 3.20–3.17 (m, 4H), 2.92–2.89 (m, 2H), 2.74–2.71 (m, 4H), 2.49–2.45 (m, 1H), 2.07–2.05 (m, 3H), 1.89–1.66 (m, 5H).^{13}C NMR (50 MHz, $CDCl_3$) δ 157.7, 148.1, 141.5, 139.2, 130.3, 128.7, 128.3, 124.4, 123.6, 121.8, 120.2, 120.1, 114.0, 67.5, 62.1, 54.8, 54.3, 53.2, 34.8, 33.8, 31.9, 29.5, 29.1, 28.9, 27.8, 23.4, 22.6. IR (neat, cm^{-1}): 3400, 3018, 2927, 2399, 1602, 1384, 1215, 1084, 928, 758, 669. ESI-MS: (m/z) = 367 $[M + H]^+$. HRMS (ESI) exact mass calcd for $[C_{23}H_{31}N_2O_2 + H]^+$ 367. 2386, found 367.2378.

1-(6-(Dibenzo[*b*,*f*][1,4]oxazepin-10(11*H*)-yl)-2-hydroxyhexyl)-piperidin-4-ol (48). Colourless viscous liquid (142 mg, 72%).

^{1}H NMR (300 MHz, $CDCl_3$) δ 7.40–7.34 (m, 1H), 7.24–7.14 (m, 4H), 7.04–6.99 (m, 1H), 6.87–6.80 (m, 2H), 4.47 (s, 2H), 3.82–3.75 (m, 2H), 3.60 (s, 1H), 3.28–3.20 (m, 2H), 3.00–2.98 (m, 1H), 2.77–2.75 (m, 2H), 2.50–2.41 (m, 3H), 2.39–1.96 (m, 6H), 1.71–1.66 (m, 4H). ^{13}C NMR (50 MHz, $CDCl_3$) δ 158.1, 148.4, 141.8, 139.6, 130.8, 129.1, 128.7, 124.8, 124.0, 122.2, 120.5, 114.4, 66.7, 55.2, 54.2, 53.4 51.1, 48.8, 35.27, 34.6, 34.18, 32.28, 30.05, 29.8, 29.7, 29.5, 29.3, 28.3, 23.5. IR (neat, cm^{-1}): 3401, 3019, 2936, 2399, 1601, 1487, 1384, 1215, 1059, 928, 757, 669. ESI-MS: (m/z) = 397 $[M + H]^+$. HRMS (ESI) exact mass calcd for $[C_{24}H_{33}N_2O_3 + H]^+$ 397.2491, found 397.2487.

Abbreviations

MtbLigA	*M. tuberculosis* LigA
ATP	Adenosine triphosphate
NAD^+	Nicotinamide adenine dinucleotide
MIC	Minimum inhibitory concentration
EtBr	Ethidium bromide

Acknowledgements

T. K. and N. Y. are recipients of CSIR senior research fellowships. The study was funded by the Council of Scientific and Industrial Research, India, through SPLenDID [BSC0113] and GENESIS [BSC0104] grants, respectively.

This manuscript bears the CSIR-CDRI communication number 8952.

Notes and references

1 M. Jassal and W. R. Bishai, *Lancet Infect. Dis.*, 2009, **9**, 19–30.
2 K. Duncan and C. E. Barry 3rd, *Curr. Opin. Microbiol.*, 2004, **7**, 460–465.
3 Y. L. Janin, *Bioorg. Med. Chem.*, 2007, **15**, 2479–2513.
4 R. P. Lange, H. H. Locher, P. C. Wyss and R. L. Then, *Curr. Pharm. Des.*, 2007, **13**, 3140–3154.
5 T. Khanam and R. Ramachandran, *J. Indian Inst. Sci.*, 2014, **94**, 149–168.
6 M. A. Petit and S. D. Ehrlich, *Nucleic Acids Res.*, 2000, **28**, 4642–4648.
7 A. Wilkinson, J. Day and R. Bowater, *Mol. Microbiol.*, 2001, **40**, 1241–1248.
8 V. Sriskanda and S. Shuman, *J. Biol. Chem.*, 2002, **277**, 9661–9667.
9 J. Lu, J. Tong, H. Feng, J. Huang, C. L. Afonso, D. L. Rock, F. Barany and W. Cao, *Biochim. Biophys. Acta*, 2004, **1701**, 37–48.
10 M. Korycka-Machala, E. Rychta, A. Brzostek, H. R. Sayer, A. Rumijowska-Galewicz, R. P. Bowater and J. Dziadek, *Antimicrob. Agents Chemother.*, 2007, **51**, 2888–2897.
11 S. Shuman, *Structure*, 2004, **12**, 1335–1336.
12 A. E. Tomkinson, S. Vijayakumar, J. M. Pascal and T. Ellenberger, *Chem. Rev.*, 2006, **106**, 687–699.
13 P. J. O'Brien and T. Ellenberger, *J. Biol. Chem.*, 2004, **279**, 9750–9757.
14 M. R. Singleton, K. Hakansson, D. J. Timson and D. B. Wigley, *Structure*, 1999, **7**, 35–42.
15 K. S. Gajiwala and C. Pinko, *Structure*, 2004, **12**, 1449–1459.
16 J. Y. Lee, C. Chang, H. K. Song, J. Moon, J. K. Yang, H. K. Kim, S. T. Kwon and S. W. Suh, *EMBO J.*, 2000, **19**, 1119–1129.
17 S. K. Srivastava, R. P. Tripathi and R. Ramachandran, *J. Biol. Chem.*, 2005, **280**, 30273–30281.
18 S. Han, J. S. Chang and M. Griffor, *Acta Crystallogr., Sect. F: Struct. Biol. Cryst. Commun.*, 2009, **65**, 1078–1082.
19 M. Odell, V. Sriskanda, S. Shuman and D. B. Nikolov, *Mol. Cell*, 2000, **6**, 1183–1193.
20 T. Ellenberger and A. E. Tomkinson, *Annu. Rev. Biochem.*, 2008, **77**, 313–338.
21 A. J. Doherty and S. W. Suh, *Nucleic Acids Res.*, 2000, **28**, 4051–4058.
22 J. Nandakumar, P. A. Nair and S. Shuman, *Mol. Cell*, 2007, **26**, 257–271.
23 J. M. Pascal, P. J. O'Brien, A. E. Tomkinson and T. Ellenberger, *Nature*, 2004, **432**, 473–478.
24 N. Dwivedi, D. Dube, J. Pandey, B. Singh, V. Kukshal, R. Ramachandran and R. P. Tripathi, *Med. Res. Rev.*, 2008, **28**, 545–568.
25 S. D. Mills, A. E. Eakin, E. T. Buurman, J. V. Newman, N. Gao, H. Huynh, K. D. Johnson, S. Lahiri, A. B. Shapiro, G. K. Walkup, W. Yang and S. S. Stokes, *Antimicrob. Agents Chemother.*, 2011, **55**, 1088–1096.
26 S. S. Stokes, M. Gowravaram, H. Huynh, M. Lu, G. B. Mullen, B. Chen, R. Albert, T. J. O'Shea, M. T. Rooney, H. Hu, J. V. Newman and S. D. Mills, *Bioorg. Med. Chem. Lett.*, 2012, **22**, 85–89.
27 S. S. Stokes, H. Huynh, M. Gowravaram, R. Albert, M. Cavero-Tomas, B. Chen, J. Harang, J. T. Loch 3rd, M. Lu, G. B. Mullen, S. Zhao, C. F. Liu and S. D. Mills, *Bioorg. Med. Chem. Lett.*, 2011, **21**, 4556–4560.
28 W. Gu, T. Wang, F. Maltais, B. Ledford, J. Kennedy, Y. Wei, C. H. Gross, J. Parsons, L. Duncan, S. J. Arends, C. Moody, E. Perola, J. Green and P. S. Charifson, *Bioorg. Med. Chem. Lett.*, 2012, **22**, 3693–3698.
29 G. Ciarrocchi, D. G. MacPhee, L. W. Deady and L. Tilley, *Antimicrob. Agents Chemother.*, 1999, **43**, 2766–2772.
30 H. Brotz-Oesterhelt, I. Knezevic, S. Bartel, T. Lampe, U. Warnecke-Eberz, K. Ziegelbauer, D. Habich and H. Labischinski, *J. Biol. Chem.*, 2003, **278**, 39435–39442.
31 L. Haracska, R. E. Johnson, I. Unk, B. Phillips, J. Hurwitz, L. Prakash and S. Prakash, *Mol. Cell. Biol.*, 2001, **21**, 7199–7206.
32 D. K. Singh, S. Krishna, S. Chandra, M. Shameem, A. L. Deshmukh and D. Banerjee, *Med. Res. Rev.*, 2014, **34**, 567–595.
33 W. J. Gui, S. Q. Lin, Y. Y. Chen, X. E. Zhang, L. J. Bi and T. Jiang, *Biochem. Biophys. Res. Commun.*, 2011, **405**, 272–277.

34 S. K. Srivastava, D. Dube, V. Kukshal, A. K. Jha, K. Hajela and R. Ramachandran, *Proteins*, 2007, **69**, 97–111.
35 S. K. Srivastava, D. Dube, N. Tewari, N. Dwivedi, R. P. Tripathi and R. Ramachandran, *Nucleic Acids Res.*, 2005, **33**, 7090–7101.
36 P. J. Luncsford, B. A. Manvilla, D. N. Patterson, S. S. Malik, J. Jin, B. J. Hwang, R. Gunther, S. Kalvakolanu, L. J. Lipinski, W. Yuan, W. Lu, A. C. Drohat, A. L. Lu and E. A. Toth, *DNA Repair*, 2013, **12**, 1043–1052.
37 I. I. Dianova, V. A. Bohr and G. L. Dianov, *Biochemistry*, 2001, **40**, 12639–12644.
38 R. A. Bennett, D. M. Wilson 3rd, D. Wong and B. Demple, *Proc. Natl. Acad. Sci. U. S. A.*, 1997, **94**, 7166–7169.
39 V. Kukshal, M. Mishra, A. Ajay, T. Khanam, R. Sharma, D. Dube, D. Chopra, R. P. Tripathi and R. Ramachandran, *MedChemComm*, 2012, **3**, 453–461.
40 S. K. Srivastava, R. P. Tripathi and R. Ramachandran, *J. Biol. Chem.*, 2005, **280**, 30273–30281.
41 H. Brotz-Oesterhelt, I. Knezevic, S. Bartel, T. Lampe, U. Warnecke-Eberz, K. Ziegelbauer, D. Habich and H. Labischinski, *J. Biol. Chem.*, 2003, **278**, 39435–39442.
42 M. Lavesa-Curto, H. Sayer, D. Bullard, A. MacDonald, A. Wilkinson, A. Smith, L. Bowater, A. Hemmings and R. P. Bowater, *Microbiol.*, 2004, **150**, 4171–4180.
43 A. Wilkinson, H. Sayer, D. Bullard, A. Smith, J. Day, T. Kieser and R. Bowater, *Proteins*, 2003, **51**, 321–326.
44 Z. J. Ren, R. G. Baumann and L. W. Black, *Gene*, 1997, **195**, 303–311.
45 U. E. Park, B. M. Olivera, K. T. Hughes, J. R. Roth and D. R. Hillyard, *J. Bacteriol.*, 1989, **171**, 2173–2180.
46 G. G. Wilson and N. E. Murray, *J. Mol. Biol.*, 1979, **132**, 471–491.
47 C. Gong, A. Martins, P. Bongiorno, M. Glickman and S. Shuman, *J. Biol. Chem.*, 2004, **279**, 20594–20606.
48 G. Ciarrocchi, D. G. MacPhee, L. W. Deady and L. Tilley, *Antimicrob. Agents Chemother.*, 1999, **43**, 2766–2772.
49 T. A. Ranalli, S. Tom and R. A. Bambara, *J. Biol. Chem.*, 2002, **277**, 41715–41724.
50 S. Tom, L. A. Henricksen and R. A. Bambara, *J. Biol. Chem.*, 2000, **275**, 10498–10505.
51 D. J. Hosfield, C. D. Mol, B. Shen and J. A. Tainer, *Cell*, 1998, **95**, 135–146.